North Equatorial Current Influence on Ocean Mixing Dynamics in the Western Tropical Pacific Along the 149 E Transect

Mei Ettari

University of Washington

School of Oceanography, Box 355351

Seattle, WA 98195-5351

mettari@uw.edu

14 March 2025

Abstract

This study examines the relationship between the strength of the North Equatorial Current (NEC) and local ocean mixing along the 149 E transect from 4 N to 16 N. Data was collected in the Western Tropical Pacific aboard the R/V *Thomas G. Thompson* from 29 December 2024 to 10 January 2025 using an Acoustic Doppler Current Profiler (ADCP) and Conductivity-Temperature-Depth (CTD) sensor. Zonal velocity data from the upper 700 m revealed distinct eastward and westward velocity patterns. The NEC was present from 8 N to 16 N, with peak velocities between 9 N and 12 N in the upper 200 m. The North Equatorial Counter Current (NECC) was observed between 4 N and 6 N in the upper 200 m. Zonal jets were noted at 10 N to 11 N and 13 N to 14 N, with an eddy observed at 15 N. The mixed layer depth (MLD) averaged 82 m across the transect. Although no clear relationship between MLD and NEC strength was found, velocity patterns suggested significant variations in mixing and stratification. Depth profiles of buoyancy frequency (N^2), shear magnitude, and Richardson number (Ri) highlighted regions of shear-driven turbulence, particularly where Ri values fell below 0.25, indicating potential vertical mixing. This effect was predominantly observed in the mixed layer, with only one station showing deeper ocean mixing. The shear in the region was not strong enough to overcome buoyancy forces, suggesting a strongly stratified water column that inhibits vertical mixing. These findings underscore the need for further research on the NEC's impact on shear and buoyancy interactions in ocean mixing dynamics.

Plain Language Summary

This study examines the relationship between the strength of the North Equatorial Current (NEC) and local ocean mixing along the 149 E transect from 4 N to 16 N. Data was collected aboard the R/V Thomas G. Thompson from 29 December 2024 to 10 January 2025 in the Western Tropical Pacific using instruments that measure ocean current speeds and water properties. The study found that the NEC was strongest between 9 N and 12 N. Other currents, like the North Equatorial Counter Current (NECC), and small whirlpools called eddies, were also present along the transect at varying latitudes.

This study also examined the mixed layer depth (MLD), the upper part of the ocean where water properties are homogenous and mixed by currents and wind. On average, the MLD was about 82 meters deep. While no clear link was found between the strength of the NEC and MLD, velocity patterns revealed areas with more mixing and layering. Some parts of the water column at different sampling stations showed signs of turbulence, where water mixed more vertically, particularly in the upper layer. However, these observations were not significant enough to contribute to substantial results. In most areas, the mixing wasn’t strong enough to affect deeper parts of the ocean, suggesting that the ocean's layers are strongly separated, inhibiting deeper mixing in this region. These results highlight the need for further research into how different mixing forces interact in the ocean and influence the water column.

Introduction

Oceans play a crucial role in regulating Earth's climate, supporting marine biodiversity, and sustaining the livelihoods of millions of people. Ocean mixing redistributes heat, circulates essential nutrients for aquatic ecosystems, and helps regulate Earth's climate. Within the ocean, turbulence arises from variations in density, velocity, and vorticity, creating local gradients that drive instability in the water column (Mann, 2005). These turbulent processes promote mixing at both large and small scales, altering currents and contributing to the ocean's dynamic nature (Gargett and Mara, 2002).

Mixing is often induced by internal waves, which are generated by wind and tidal forces and driven by vertical shear—the gradient of horizontal velocity. In stratified ocean columns, shear opposes the stabilizing effect of density stratification, leading to instabilities that enhance mixing. One example is the Kelvin-Helmholtz instability, which occurs at the interface between two horizontal fluid layers with different velocities and densities (Mikhailovskii, 1982). These instabilities influence ocean currents, affecting the depth and intensity of the mixed layer.

The mixed layer, which directly interacts with the atmosphere, plays a key role in climate feedback mechanisms. It ranges from a few meters to a few hundred meters and is characterized by relatively uniform temperature, density, salinity, and nutrient levels due to turbulence driven by wind, buoyancy, and wave action (Treguier et al., 2023). Seasonal variations—such as changes in temperature, wind patterns, and rainfall—affect the mixed layer, typically deepening in winter and shoaling in spring and summer. Below this layer, increasing density stratification is marked by vertical gradients in temperature and salinity (Treguier et al., 2023). The transition to a deeper, more stratified water column is defined by the thermocline, where temperature decreases sharply, and the halocline, where salinity gradually increases (Gonzàlez-Pola et al., 2007). Changes in temperature or salinity below the mixed layer may indicate deeper ocean mixing.

In the Western Tropical Pacific, the mixed layer is highly dynamic due to changing oceanographic conditions and circulation patterns. Mixed layer dynamics are driven by buoyancy, wind, and ocean currents, which influence stratification below the MLD. Weaker currents result in a more stratified water column, inhibiting the distribution of nutrients and heat across the Pacific (Liu and Zhou, 2020). Previous studies indicate that the average mixed layer depth (MLD) in this region is approximately 29 m (Lukas and Lindstrom, 1991). Another study suggests that the annual mean MLD ranges between 40 m and 70 m around 15 N and 150 E (Qu, 2003).

One of the most important currents in the Western Tropical Pacific is the North Equatorial Current (NEC), a westward-flowing current driven by trade winds. The NEC is part of the North Pacific subtropical gyre and typically flows between 8 N and 18 N (Liu and Zhou, 2020). South of the NEC lies the North Equatorial Counter Current (NECC), which flows eastward at lower latitudes, between 2 N and 10 N, near the equator and above the South Pacific Ocean gyre (Sun et al., 2019). As the NEC approaches the Philippines, it bifurcates into two major currents: the Kuroshio Current to the north and the Mindanao Current to the south.

The exact depth of the NEC remains a subject of debate among researchers. Some studies suggest depths between 400 and 500 m (Li and Gan, 2023), while others indicate depths of 200 to 400 m (Wang et al., 2019). Hu and Hu (2014) found that the upper 200 m, containing the mixed layer, accounts for more than 70% of total NEC transport and exhibits the strongest interannual variability compared to deeper layers. Their study also determined that the bottom of the NEC extends beyond 400 m. Other research has shown that the NEC's maximum mean zonal velocity, which occurs primarily between 10.5 N and 15.5 N, ranges from -0.165 m/s to -0.30 m/s at a depth of approximately 70 m (Zhang et al., 2017). The NEC's shifting conditions and variability make it challenging to determine its precise depth and velocity, underscoring its complex role in ocean circulation.

This study aims to address existing uncertainties regarding the NEC by testing the hypothesis that its strength is directly correlated with the intensity of local mixing. Specifically, it proposes that an increase in the strength of the NEC in the Western Tropical Pacific influences water column stratification and enhances vertical mixing through variations in buoyancy, shear, and turbulence within the upper ocean.

Methods

3.1 Instrumentation and Sampling Strategy

Research was conducted in the Western Tropical Pacific onboard the R/V *Thomas G. Thompson* from 29 December 2024 to 10 January 2025. The primary focus included data collection using the Sea-Bird SBE-911 plus Conductivity, Temperature, and Depth (CTD) sensor and the 75 kHz Ocean Surveyor (OS75) underway hull-mounted Acoustic Doppler Current Profiler (ADCP). The CTD reached 1000 m depths to ensure that the data included both the North Equatorial Current (NEC) and the mixed layer. The ADCP operated continuously along the transect, measuring the speed and direction of the currents.

The transect was conducted along 149 E, from 4 N to 16 N. A total of 13 CTD casts were spaced 1 degree apart (Table 1, Fig. 1). These locations were selected based on the previously proposed cruise transect and the NEC's flow pattern.

Table 1.

Sampling Station Numbers Along Transect 149 E From 5 N - 15 N.

Station #	Latitude (ºN)
8A	4
8	5
9	6
10	7
11	8
12	9
13	10
14	11
15	12
16	13
17	14
18	15
19	16

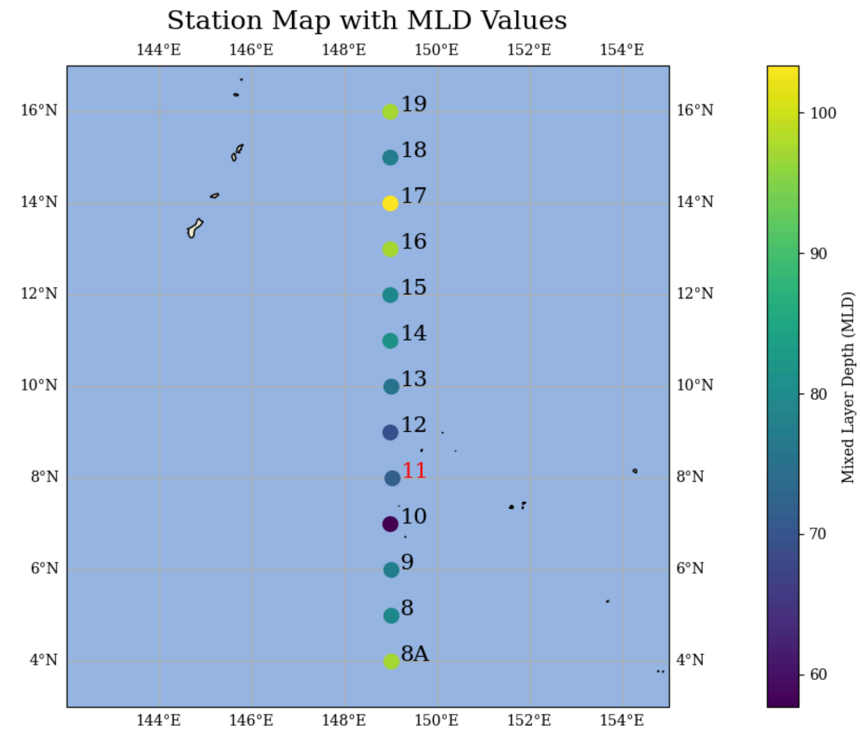

Figure 1. Location of the transect along 149 E, extending from 4 N to 16 N, with 13 CTD stations spaced 1 degree apart, labeled Station 8A through Station 19. Each station is represented by a contour dot, indicating its corresponding mixed layer depth (MLD). The Caroline Islands' topography is between 6 N and 9 N. Station 11 is positioned slightly farther east at 149.027 E due to shallower waters encountered at its original location.

3.2 Quantifying Mixing

CTD data collected during the cruise were processed in Python using Google Colab. The "ctd" Python package was used to load and analyze the raw data, which included pressure (dbar), temperature (°C), and salinity (PSU). Potential density was calculated using the Gibbs Seawater (GSW) Oceanographic Toolbox (McDougall and Barker, 2011), referencing a surface pressure of 0 dbar. The MLD was determined using a threshold method, where the depth at which all the following conditions were met relative to a reference value of 10 dbar: a temperature decrease of more than 0.2 °C, a salinity increase of more than 0.1 PSU, and a potential density increase of more than 0.03 kg/m^3. A MLD value was returned where all conditions were met (Example profile from Station 19, Fig. 2)

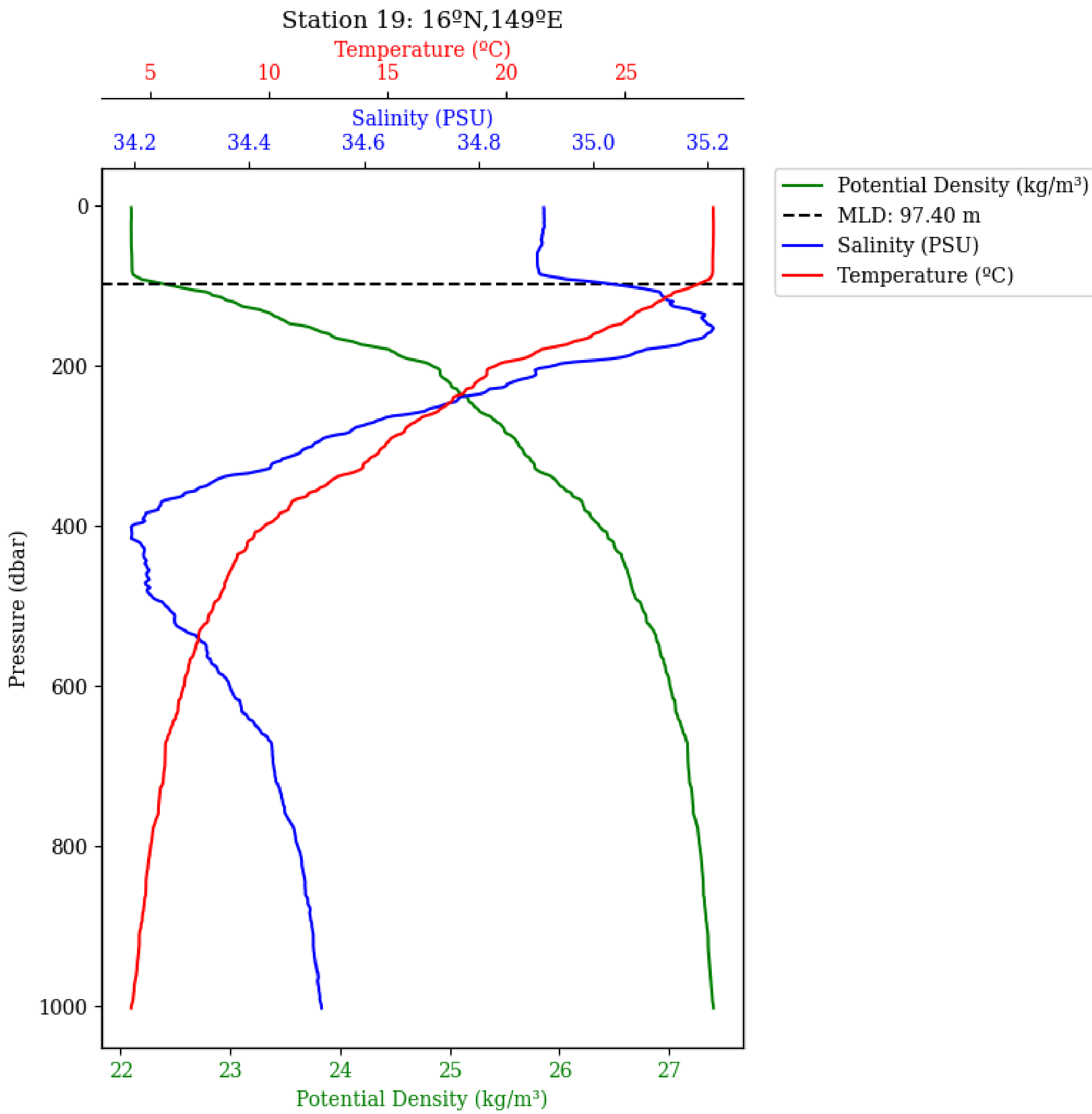

Figure 2. Depth profile at Station 19: 16 N, 149 E. Potential density (green), salinity (blue), and temperature (red) are plotted against pressure. The Mixed layer depth (MLD) (black dashed line) was calculated where potential density, salinity, and temperature meet the threshold conditions.

To mathematically assess mixing and its location in the water column, the buoyancy frequency (N^2), zonal (du/dz) and meridional (dv/dz) velocity shear, and the magnitude of the shear vector ($\sqrt{((du/dz)^2 + (dv/dz)^2)}$) were calculated from the CTD and ADCP data using the GSW toolbox. N^2 values were smoothed by calculating the cumulative sum of the data and then taking the running mean. These values allowed for the computation of the Richardson Number ($Ri = N^2/(du/dz)^2$) at all stations, which indicates where there is potential shear-driven mixing in the water column (Miles, 1961). An Ri value $< \frac{1}{4}$ indicates reduced stratification and some vertical mixing, while an Ri value $> \frac{1}{4}$ indicates that the water column is more stratified, resulting in turbulent mixing being suppressed (Miles, 1961).

Results

The zonal velocity in the upper 700 m was analyzed along 149 E from 4 N to 16 N (Fig. 3). Between 6.5 N and 9 N, no significant velocity fluctuations were observed, with an average zonal velocity of -0.022 m/s. Oscillations between eastward and westward velocity occurred along the transect from 200 m to 700 m, with an average velocity of -0.021 m/s. Notably, a strong eastward velocity was present between 10 N and 11 N from 200 m to 700 m, averaging 0.067 m/s. Another region of strong eastward velocity was observed between 13 N and 14 N from 300 m to 700 m, with an average velocity of 0.104 m/s.

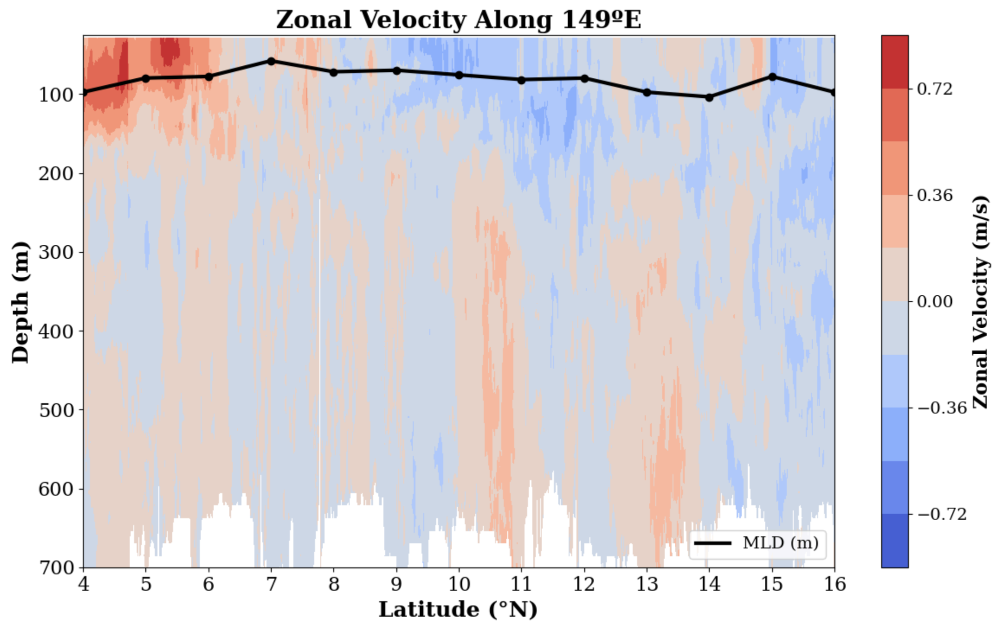

Figure 3. Contour plot of east-west zonal velocity along 149 E from 4 N to 16 N, including the mixed layer depth (MLD) from Station 8A (4 N) to Station 19 (16 N), plotted against depth in the upper 700 m. Positive values represent eastward velocity, while negative values indicate westward velocity. The eastward velocity from 4 N to 6 N corresponds to the North Equatorial Countercurrent (NECC). The westward velocity from 8 N to 16 N is associated with the North Equatorial Current (NEC), with the strongest velocities occurring between 9 N and 12 N. Below 200 m, equatorial deep jets are observed between 10 N-11 N and 13 N–14 N.

Zonal velocity and magnitude exhibited the largest fluctuations in the upper water column (Fig. 4, 5). From 4 N to 6 N, eastward velocity dominated the upper 160 m, with an average velocity of 0.37 m/s, indicated by a distinct velocity magnitude range from 0 m/s to 1.19 m/s. At 6 N, the eastward velocity dissipated, and between 6 N and 6.5 N, it approached 0 m/s. Westward velocity emerged in the upper water column at 6.5 N. Between 7 N and 8 N, zonal velocity again approached 0 m/s, while westward velocity became prominent throughout the water column from 8 N to 16 N. Notably, between 9 N and 12 N, westward velocity and magnitude were most substantial from the surface to 175 m, with a maximum velocity of -0.795 m/s. At 15 N, an eastward velocity appeared but quickly transitioned to a westward velocity, coinciding with the shoaling of the MLD. Where the MLD deepened or shoaled, velocity varied with depth (Fig. 4). While the MLD fluctuated with latitude, it remained relatively stable above 100 m, averaging 82 m.

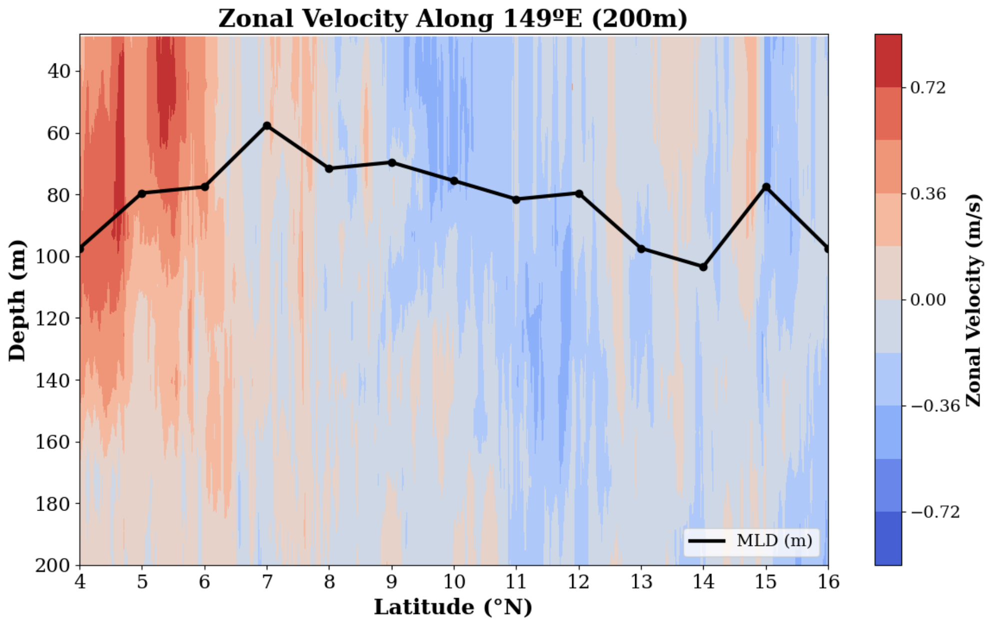

Figure 4. Contour plot of east-west zonal velocity along 149 E from 4 N to 16 N, including the mixed layer depth (MLD) from Station 8A (4 N) to Station 19 (16 N), plotted against depth in the upper 200 m. Positive values represent eastward velocity, while negative values indicate westward velocity. The eastward velocity from 4 N to 6 N aligns with the North Equatorial Countercurrent (NECC), while the westward velocity from 8 N to 16 N is associated with the North Equatorial Current (NEC).

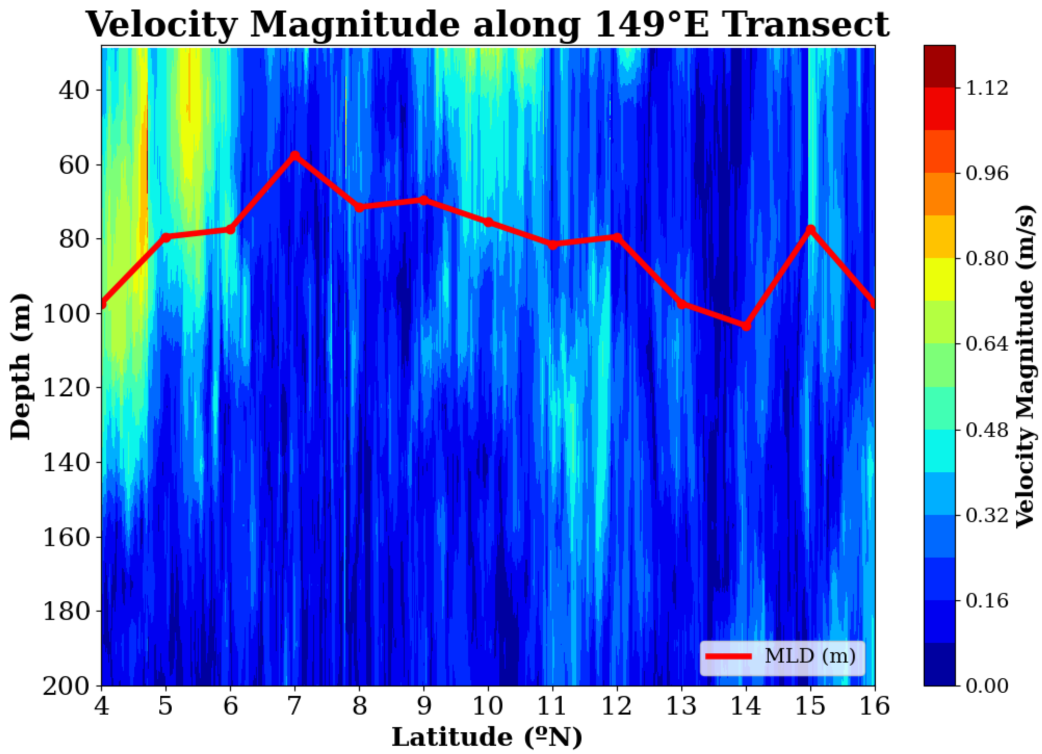

Figure 5. Contour plot of velocity magnitude along 149 E from 4 N to 16 N, including the mixed layer depth (MLD) in red from Station 8A (4 N) to Station 19 (16 N), plotted against depth in the upper 200 m. The strongest velocity magnitudes correspond to the North Equatorial Counter Current (NECC) from 4 N to 6 N and the North Equatorial Current (NEC) from 9 N to 12 N.

Depth profiles of buoyancy frequency (N^2), shear magnitude, and the Richardson number (Ri) were computed and plotted for each station (example for Station 19, Fig. 6). N^2 values varied but remained mostly positive from the surface to depth, indicating a stable, well-stratified water column, with the highest N^2 values just below the mixed layer (Fig. 7). However, at 10 N and 11 N, N^2 values approached negative at depths shallower than 70 m, suggesting weaker and less stable stratification. Within the mixed layer, N^2 values remained close to zero, marking the transition where the mixed layer ends. The highest N^2 values across all stations occurred below the MLD, between 90 m and 350 m, before decreasing toward zero with depth. Near-zero N^2 values, combined with high shear magnitudes, corresponded to Ri values below 0.25, indicating potential vertical mixing. This was observed within the mixed layer at 5 N, 7 N, 9 N, 10 N, 12 N, 13 N, 14 N, and 16 N. Below 250 m, deeper mixing was only observed at 6 N.

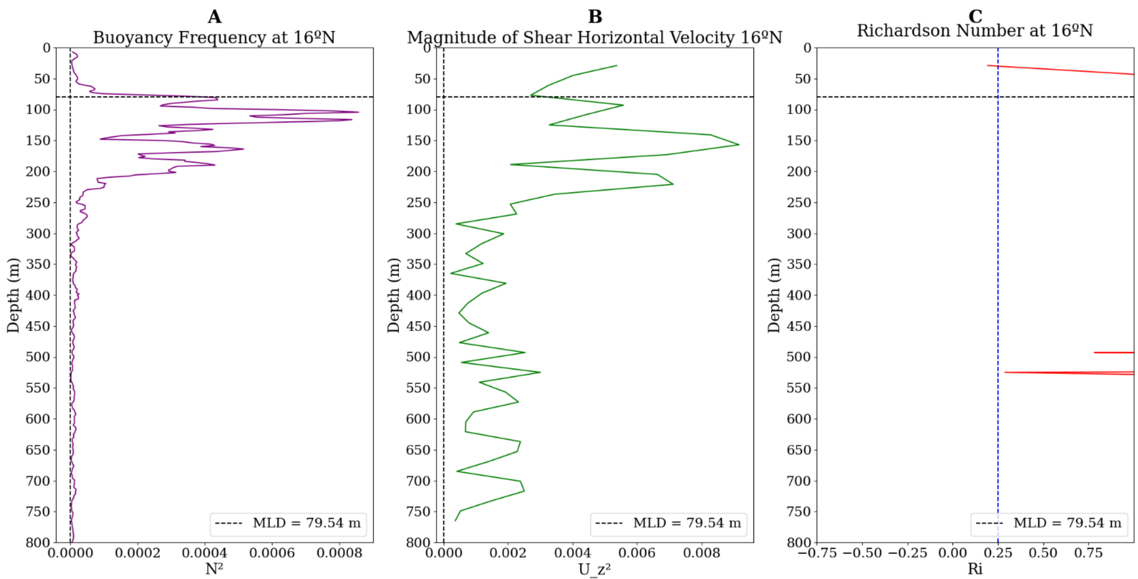

Figure 6. Station 19 (16 N) displays (A) the vertical profile of buoyancy frequency (N^2), where higher positive values indicate a stable, stratified water column; (B) Magnitude of shear horizontal velocity; and (C) Richardson number, which highlights the relative importance of buoyancy forces versus shear forces, providing insight into potential turbulence and mixing within the water column. Values to the left of the blue dotted line ($Ri < 0.25$) indicate conditions favorable for vertical mixing. When shear velocity magnitude is high and buoyancy frequency is low, overturning in the water column can occur, enhancing vertical mixing. For simplicity, only Station 19 is plotted here, though all stations were analyzed separately.

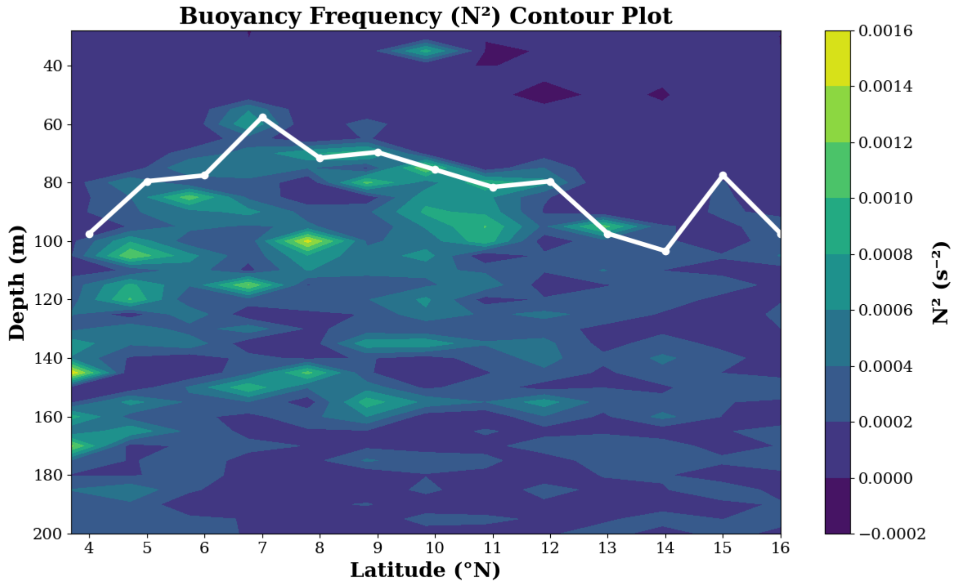

Figure 7. Contour plot of buoyancy frequency plotted against depth in the upper 300 m, including the mixed layer depth (MLD) at each latitude. Higher values indicate increased stratification, marking the transition from the mixed layer to a more stratified water column. Values closer to 0 suggest a less stratified region.

Discussion

The location and zonal velocity averages of the NEC align with previous literature, confirming its presence from 8 N to 16 N along 149 E, with the strongest NEC velocities occurring between 9 N and 12 N. While the exact depth of the NEC remains uncertain, previous studies suggest it is consistently found within the upper 200 m. Conversely, between 4 N and 8 N, the positive zonal velocity in the upper 200 m corresponds to the North Equatorial Countercurrent (NECC), which flows eastward, opposite to the NEC (Sun et al., 2019).

Some eastward zonal velocities observed below 200 m may indicate the presence of the North Equatorial Undercurrent (NEUC), which flows west to east beneath the NEC (Ishizaki et al., 2019). The oscillating zonal velocities observed below 200 m between 10 N and 11 N, as well as 13 N and 14 N, exhibit characteristics of alternating zonal jets known as Tsuchiya jets (Furue et al., 2009).

There does not appear to be a direct correlation between the MLD and NEC strength. The shallowest MLD was observed at 7 N, likely influenced by the topography of the Caroline Islands. At 8 N, the R/V *Thompson* encountered waters as shallow as 42 m and had to adjust its sampling location eastward. The average MLD during sampling was 82 m, though it likely fluctuates due to changing oceanographic conditions rather than the NEC at the time of sampling.

At 15 N, a distinct eastward velocity surrounded by westward velocities suggests the presence of a cyclonic eddy, supported by the shoaling of the MLD—consistent with the characteristics of a cyclonic eddy in the Northern Hemisphere (Gaube, McGillicuddy, & Moulin, 2019; Fig. 4).

Across all stations, the water column was well-stratified and stable below the MLD, marking a threshold where stratification was strongest and vertical mixing was inhibited (Fig. 6). However, in regions where Ri values dropped below ¼, potential vertical mixing was observed, indicating that localized shear-driven turbulence may contribute to breaking stratification and enhancing mixing. Along the transect, Ri values reaching the critical threshold were primarily found within the mixed layer, with deeper mixing occurring at only one station. The Ri values did not show a clear relationship between the deepening of the MLD and the NEC, highlighting that shear forces were not strong enough to overcome the stabilizing effect buoyancy plays in the water column within this region. Additionally, buoyancy and shear provide further insight into upper water column stratification, which can help explain MLD variability on a broader scale. These localized processes play a significant role in global ocean circulation and mixing.

Conclusion

This study enhances our understanding of how the North Equatorial Current (NEC) influences local ocean mixing in the Western Tropical Pacific. The observed patterns generally align with previous research, however further investigation is needed to refine our knowledge of NEC variability, its impact on global circulation, and its role in upper-ocean mixing and stratification.

The NEC, which extends along 149 E between 8 N and 16 N, exhibits its highest velocities between 9 N and 12 N. It is most significant in the upper 200 meters, though zonal velocities have been observed as deep as 700 meters at various latitudes along the transect. The North Equatorial Countercurrent (NECC) is present between 4 N and 6 N in the upper 200 meters, while zonal jets are observed at 10 N to 11 N and 13 N to 14 N, with an eddy present at 15 N.

Despite these detailed observations, no significant relationship was found between the strength of the NEC and mixed layer depth (MLD). However, potential vertical mixing was identified in areas where the Richardson number (Ri) dropped below its critical value of ¼, indicating shear-driven turbulence may contribute to instability, break stratification, and promote mixing. This effect–though predominantly observed in the mixed layer–was not significant across most of the transect, with only one station showing potential deeper ocean mixing.

Furthermore, the shear in the region was not strong enough to overturn buoyancy forces, suggesting that the water column is strongly stratified and inhibits vertical mixing below the MLD.

This study highlights the dynamic nature of the MLD, with notable variations observed across the 149 E transect. These findings emphasize the need for further measurements of the MLD under varying oceanographic conditions to better understand the factors influencing its variability. While the data generally aligns with existing research on the NEC and MLD, additional studies are needed to fully characterize the influence of NEC variability on global ocean circulation, particularly in terms of vertical mixing and stratification. The interaction between shear and buoyancy forces plays a crucial role in ocean dynamics in the Western Tropical Pacific, and understanding this relationship can provide valuable insights into global ocean processes.

Acknowledgments

Thank you to the captain, officers, crew, and chief scientists aboard the R/V *Thompson* for their assistance and support throughout our research collection. A warm special appreciation goes to the marine technicians who worked tirelessly to ensure that all on-deck operations and data collection went smoothly. Thank you to all the oceanography seniors who participated in aiding in data collection and analyses, as well as being moral support throughout the entire senior thesis process. Thank you to the University of Washington School of Oceanography for providing us with this once-in-a-lifetime opportunity. To our amazing and dedicated instructors—Ginger Armbrust, Alison Gray, Andrea Ogston, François Ribalet, and Mark Warner—thank you for your continued guidance and support.

References

Furue, R., McCreary, J. P., Jr., & Yu, Z. (2009). Dynamics of the Northern Tsuchiya Jet. *Journal of Physical Oceanography, 39*(9), 2024-2051. https://doi.org/10.1175/2009JPO4065.1

Gargett, A., & Marra, J. O. H. N. (2002). Effects of upper ocean physical processes (turbulence, advection and air-sea interaction) on oceanic primary production. *The Sea, 12*, 19-49.

Gaube, P., McGillicuddy, D. J., & Moulin, A. J. (2019). Mesoscale Eddies Modulate Mixed Layer Depth Globally. *Geophysical Research Letters, 46*(3), 1505-1512. https://doi.org/10.1029/2018GL080006

González-Pola, C., Freeland, H., Valdés, L., Chu, P. C., Daniel, C., Hogg, N. G., Jenkins, G. M., Kara, A. B., & Lavín, A. (2007). Vertical structure of the upper ocean from profiles fitted to physically consistent functional forms. *Deep Sea Research Part I: Oceanographic Research Papers*. https://doi.org/10.1016/j.dsr.2007.07.003

Ishizaki, H., Nakano, T., Nakano, H., et al. (2019). Interdecadal variability of the North Equatorial Undercurrent (NEUC) found in the long-term hydrographic observations along 137 E. *Journal of Oceanography, 75*, 395–414. https://doi.org/10.1007/s10872-019-00509-6

Li, J., & Gan, J. (2023). How the forcing dynamics of the western boundary currents in the Pacific respond to the North Equatorial Current. *Progress in Oceanography, 210*, 102950. https://doi.org/10.1016/j.pocean.2022.102950

Liu, X., & Zhou, H. (2020). Seasonal Variations of the North Equatorial Current Across the Pacific Ocean. *Journal of Geophysical Research: Oceans, 125*(6), e2019JC015895. https://doi.org/10.1029/2019JC015895

Lukas, R., & Lindstrom, E. (1991). The mixed layer of the western equatorial Pacific Ocean. *Journal of Geophysical Research: Oceans, 96*(S01), 3343-3357. https://doi.org/10.1029/90JC01951

Mann, K. H., & Lazier, J. R. (2005). *Dynamics of marine ecosystems: biological-physical interactions in the oceans*. John Wiley and Sons.

Mikhailovskii, A. B. (1982). Hydrodynamic theory of drift Kelvin–Helmholtz instabilities. *Journal of Plasma Physics, 28*(1), 1–11. https://doi.org/10.1017/S0022377800000039

Qiu, B., & Chen, S. (2010). Interannual-to-Decadal Variability in the Bifurcation of the North Equatorial Current off the Philippines. *Journal of Physical Oceanography, 40*(11), 2525-2538. https://doi.org/10.1175/2010JPO4462.1

Qiu, B., Rudnick, D. L., Cerovecki, I., Cornuelle, B. D., Chen, S., Schönau, M. C., McClean, J. L., & Gopalakrishnan, G. (2015). The Pacific North Equatorial Current: New insights from the origins of the Kuroshio and Mindanao Currents (OKMC) Project. *Oceanography, 28*(4), 24–33. https://doi.org/10.5670/oceanog.2015.78

Qu, T. (2003). Mixed layer heat balance in the western North Pacific. *Journal of Geophysical Research: Oceans, 108*(C7). https://doi.org/10.1029/2002JC001536

Treguier, A. M., et al. (2023). The mixed-layer depth in the Ocean Model Intercomparison Project (OMIP): impact of resolving mesoscale eddies. *16*(13).

Wang, F., Wang, Q., Zhang, L., Hu, D., Hu, S., & Feng, J. (2019). Spatial distribution of the seasonal variability of the North Equatorial Current. *Deep Sea Research Part I: Oceanographic Research Papers, 144*, 63-74. https://doi.org/10.1016/j.dsr.2019.01.001

Zhang, L., Wang, F. J., Wang, Q., Hu, S., Wang, F., & Hu, D. (2017). Structure and Variability of the North Equatorial Current/Undercurrent from Mooring Measurements at 130 E in the Western Pacific. *Scientific Reports, 7*(1), 1-9. https://doi.org/10.1038/srep46310